Frontiers in Bioscience Landmark

Front. Biosci. (Landmark Ed) **2024**; 29(2): 48
https://doi.org/10.31083/j.fbl2902048

Original Research

PPP3CB Inhibits Cell Proliferation and the Warburg Effect in Bladder Cancer by Blocking PDHK1

Xiangmin Qiu[1,†], Ziqing Jiang[1,†], Yu Luo[2,†], Dayu Tian[1], Tao Song[2,*], Qianyin Li[1,*]

[1]The Ministry of Education Key Laboratory of Laboratory Medical Diagnostics, The College of Laboratory Medicine, Chongqing Medical University, 400016 Chongqing, China
[2]Department of Laboratory Medicine, Chongqing Health Center for Women and Children, Women and Children's Hospital of Chongqing Medical University, 400016 Chongqing, China
*Correspondence: CQSFYsongtao@163.com (Tao Song); liqianyin904@cqmu.edu.cn (Qianyin Li)
[†]These authors contributed equally.
Academic Editor: Amancio Carnero Moya
Submitted: 20 June 2023 Revised: 31 October 2023 Accepted: 17 November 2023 Published: 4 February 2024

Abstract

Background: Cancer treatment has recently shifted towards metabolic approaches aimed at enhancing therapeutic efficacy. Somewhat surprisingly, a known regulator of energy metabolism in normal tissues, *PPP3CB*, is down-regulated in bladder cancer. This suggests that *PPP3CB* could exert an inhibitory effect on bladder cancer through its role in energy metabolism. **Methods**: To explore the above hypothesis, we employed non-targeted metabolism screening in bladder cancer cells with knockdown of *PPP3CB*. Glucose uptake and lactate production were carefully measured using specialized assay kits for glucose/lactic acid content. Western blot analysis was also used to evaluate the expression levels of pyruvate dehydrogenase kinase 1 (PDHK1) and p-PDHA1 in cells with *PPP3CB* knockdown. To substantiate the findings, co-immunoprecipitation (co-IP) experiments were performed to validate the interaction between *PPP3CB* and PDHK1. Various *in vitro* assays were also performed, including clone formation assay and Cell Counting Kit-8 (CCK8) viability assays. The *in vivo* anti-tumor potential of *PPP3CB* in bladder cancer was also studied using a nude mouse tumorigenesis model. **Results**: Significant down-regulation of *PPP3CB* was observed in bladder tumors, and potent anti-tumor effects of *PPP3CB* were observed *in vitro*. Investigation of the underlying mechanism by which *PPP3CB* hampers glycolysis in bladder cancer cells revealed that it interacted with PDHK1 to inhibit its protein stabilization. PDHK1 thus appears to be a crucial mediator through which *PPP3CB* exerts its inhibitory effects on bladder cancer cells. **Conclusions**: In summary, *PPP3CB* exerts strong inhibitory influences on bladder cancer cell proliferation and glycolysis via its destabilization of PDHK1. These results highlight the potential of *PPP3CB* as a novel regulator of the Warburg effect. Interestingly, the downregulation of *PPP3CB* in bladder cancer cells increases the Warburg effect, thereby generating more lactic acid and reshaping the tumor microenvironment so as to promote tumor cell proliferation.

Keywords: *PPP3CB*; bladder cancer; PDHK1; glycolysis

1. Introduction

Bladder cancer is one of the most prevalent tumor types, with over 430,000 cases diagnosed annually worldwide [1]. Known risk factors for the development of bladder cancer are male sex, advanced age and cigarette smoking [2]. Most cancers are characterized by high rates of glucose metabolism and glycolysis. During tumor growth, cells at the center of the tumor become hypoxic and oxidative phosphorylation (OXPHO) decreases [3]. This aerobic, glycolysis-dependent metabolism is referred to as the Warburg effect [4]. Metabolomic studies have revealed that metabolites such as lactic acid, glutamate and pyruvic acid are upregulated in bladder cancer, indicating the crucial role of metabolism in bladder cancer progression. Furthermore, upregulation of genes that promote the pentose phosphate and fatty-acid synthesis pathways, together with decreased activities of AMP-activated protein kinase (AMPK) and the Krebs cycle, are characteristics of bladder cancer metabolism [5]. Several alterations in glucose metabolism have also been reported in bladder cancer. These include stimulation of GLUT-1 activity [6], upregulation of glycolysis [7], increased pyruvate metabolism and lactate production [8,9], increased expression of 6-phosphofructo-2-kinase/fructose-2,6-biphosphatase 3 (PFKFB3) [10] and steroid receptor coactivator-3 (SRC-3) [11], and increased pentose phosphate pathway activity [12].

PPP3CB is a class of serine threonine calcineurin (CN) enzymes that act by dephosphorylating substrates. Calcineurin (CN) is a heterodimer consisting of a 58–59 kDa catalytic subunit (CNA) that is bound to calmodulin, and a 19 kDa regulatory subunit (CNB) that binds Ca^{2+}. CNA is comprised of *PPP3CA*, *PPP3CB*, and *PPP3CC* [13]. Studies have shown that *PPP3CB* regulates the expression, location and activity of several target genes, including *NFAT*, *Drp1*, *GSK3β*, thereby participating in the regulation of numerous physiological and pathological processes [14,15]. *PPP3CB* expression is associated with poor prognosis in cancer due to its stimulation of *NFATC2/4* activity, as shown in neuroblastoma cells. By inhibiting CN

signaling and its effect on the immune system, *PPP3CB* has a tumor-promoting role in keratinocytes and also enhances the potential of tumor stem cells [16]. It is also a regulatory factor that affects mitochondrial dynamics and systemic energy and body weight homeostasis under environmental control [14]. Therefore, *PPP3CB* appears to have a pivotal role in the regulation of tumor development and metabolism. However, it is not yet known whether *PPP3CB* can affect the development and progression of bladder cancer through glycolysis.

Pyruvate dehydrogenase kinase (PDHK) comprises four types of tissue-specific isoforms. These are mostly located in the mitochondria, and PDHK activity can be regulated by hormones, hypoxia, nutrients, etc. [17]. PDHK is activated in hypoxic tumor microenvironments through phosphorylation of its E1 α subunit in the pyruvate dehydrogenase complex (PDC). Inhibition of PDC activity leads to the failure to convert pyruvate to acetyl-CoA in the mitochondria through oxidative decarboxylation. This stops pyruvate from entering the tricarboxylic acid cycle, thereby reducing mitochondrial function and activating the glycolysis pathway [18]. PDHK is highly expressed in many cancer types, with its expression being strongly associated with poor prognosis [19]. Knockdown of PDHK can reduce the invasiveness and growth of tumor cells and reverse the Warburg effect. This phenomenon has been reported in renal clear cell carcinoma, breast cancer and other tumor types, making it a potential target for cancer treatment [20,21]. Some important oncogenes, such as Myc and HIF, can inhibit aerobic respiration in tumor cells by upregulating PDHK transcription and enhancing glycolysis, thereby promoting tumor growth [22]. PDHK is therefore one of the most widely studied anticancer targets in the aerobic glycolysis pathway. Kim *et al*. [23] showed that periostin inhibits the invasiveness of bladder cancer via the PDHK1/Akt/mTOR signaling pathway, thus indicating a pivotal role for PDHK1 in this disease.

We reasoned that *PPP3CB* might impact the proliferation of bladder cancer cells by regulating glycolysis, with the PDC being a possible target. Here we show for the first time that downregulation and inhibition of *PPP3CB* can suppress cell proliferation glycolysis in bladder cancer. Further investigation revealed the mechanism for this *PPP3CB*-mediated suppression was via regulation of PDHK1. Co-immunoprecipitation confirmed that *PPP3CB* interacts directly with PDHK1 to promote its degradation.

2. Materials and Methods

2.1 Materials

The siRNA used in this study was obtained from GenePharma (Shanghai, China). Rabbit polyclonal antibody targeting *PPP3CB* was acquired from GeneTex (Shanghai, China). Mouse monoclonal antibodies against β-tubulin and β-actin were obtained from TransGene Biotech (Beijing, China), and mouse monoclonal antibody against GAPDH was purchased from CWBIO (Beijing, China). Rabbit polyclonal antibody against green fluorescent protein (GFP) was acquired from Abcam (Cambridge, UK), mouse polyclonal antibody against Flag was purchased from Santa Cruz Biotechnology (Dallas, TX, USA), rabbit polyclonal antibody against PDHB was purchased from Proteintech (Hubei, China), while rabbit monoclonal antibody against PDHK1 and rabbit monoclonal antibody against p-DHK1 (S293) were purchased from Cell Signaling Technology (Boston, MA, USA). Sodium dichloroacetate (DCA) was purchased from Topscience (Shanghai, China) and cycloheximide (CHX) from MCE (Dallas, TX, USA).

2.2 Cell Culture

Human bladder cancer cell lines T24 and human embryonic kidney cells HEK-293T were obtained from the American Type Culture Collections (ATCC). All cell lines were grown in Dulbecco's Modified Eagle's Medium (Gibco, Thermo Fisher Scientific, New York, NY, USA) supplemented with 10% fetal bovine serum (FBS) (Gibco, Thermo Fisher Scientific, USA) and 1% penicillin/streptomycin (PS) (Hyclone, cytiva, Logan, UT, USA). Cell lines were cultured in a humidified incubator at 37 °C and with 5% CO_2. All cell lines were validated by STR profiling and tested negative for mycoplasma.

2.3 Plasmid Construction and Primer Design

The coding sequence (CDS) for *h.PPP3CB* was amplified from complementary DNA (cDNA) obtained from HEK-293T. Forward primer: 5′-ggatccgaattc ATGGCCGCCCCGGAGCC-3′. Reverse primer: 5′-atggtggtgctcgag TCACTGGGCAGTATGGTTGCCCG-3′. For truncated variants, the reverse primer for the 1–401 truncation was: 5′-atggtggtgctcgag AATTTCAGGCTGCAGCTGAACC-3′; the forward primer for the 402–524 truncation was: 5′-ggatccgaattc ATGTGCAGCCCGGAAAGAA-3′; the reverse primer for the 1–415 truncation was: 5′-atggtggtgctcgag TCACTTGCCAATTGCTCGAATTTT-3′; the reverse and forward primers for the Δ357–415 truncation were 5′-gaagactcttgccat CATAAAATTAGGCAACCAGTAAGGA-3′ and 5′-ttgcctaattttatg ATGGCAAGAGTCTTCTCTGTTCTCA-3′, respectively.

The coding sequence (CDS) for *h.*PDHK*1* was amplified from cDNA obtained from HEK-293T cells. Forward primer: 5′-ggatccgaattc ATGAGGCTGGCGCGGCTGC-3′. Reverse primer: 5′-atggtggtgctcgag CTAGGCACTGCGGAACGTCGTCAT-3′. PCR products were cloned into CMV-GFP or CMV-FLAG vectors using EcoR*I* and Xho*I* sites. The candidate sgRNA sequence for *PPP3CB* was identified using the SYNTHEGO design tool (https://tools.synthego.com/). Primers were as follow:

(sense) 5′-caccg AAGCGAUGUGUUGGGGGGAA-3′; (anti-sense) 5′-aaac TTCCCCCCAACACATCGCTT c-3′. The PCR product was ligated into CRISPR-V2 vector using the Bsmb*I* site. The following sequence was used for *si*-RNA: *si-PPP3CB*: ACCTGCTAATACACGATACCTT.

2.4 Transfection of siRNA and Plasmid DNA, and Lentivirus Infection

Lipofectamine 2000 reagent (Invitrogen, Carlsbad, CA, USA) was used for siRNA transfection as per the manufacturer's instructions. HEK-293T cells were transiently transfected using Linear Polyethylenimine following the manufacturer's instructions. For the immunoprecipitation assay, T24 cells were transfected using Lipofectamine 3000 reagent (Invitrogen, Carlsbad, CA, USA) as recommended by the manufacturer. For lentivirus infection, the cells were grown to 50–60% confluence and subsequently treated with medium containing lentivirus. They were then harvested 48 hours after transfection and incubated overnight. Virus particles were collected and used to infect T24 cells in the presence of 8 µg/mL polybrene (Sigma, Saint Louis, MO, USA). After infection, stable clones were selected using puromycin (Invitrogen, Carlsbad, CA, USA).

2.5 Cell Counting Kit-8 (CCK8) Viability Assay

Cell proliferation assays were conducted 24 hours after transfection. Cells were seeded at a density of 2000 per well in a 96-well plate. The CCK-8 reagent was diluted with DMEM to a 10% concentration and then added to each well. The absorbance at 450 nm was measured at 24-hour intervals.

2.6 Plate Colony Formation Assay

T24 cells (1000 per well) were seeded into 6-well plates and incubated under normothermia conditions for 2 weeks, with the culture medium refreshed every 3 days. Following this, cell colonies were fixed with 4% paraformaldehyde (Sangon, Shanghai, China) for 15 minutes and subsequently stained with 0.5% crystal violet (Beyotime, Shanghai, China) for 20 minutes at room temperature. The images of colonies were recorded using a microscope (Leica, DMC5400, Wetzlar, Germany).

2.7 RNA Extraction and Real-time PCR

The isolation of total RNA from cells was carried out using Trizol reagent (Invitrogen, Carlsbad, CA, USA). cDNA synthesis was performed using an oligonucleotide primer and transcription kit (Thermo Scientific, Waltham, MA, USA). Subsequently, quantitative real-time PCR was conducted using Ultra SYBR Mixture (CWBIO, Beijing, China). All experiments were normalized to internal control (18 s). The following primer pairs were utilized for quantitative real-time PCR: human *PPP3CB*, forward: 5′-CTTGGCGATTATGTGGACAGAGG-3′, reverse: 5′-GGTGTCTGCATTCATGGTTGCC-3′. Human PDHK*1*, forward: 5′-CATGTCACGCTGGGTAATGAGG-3′, reverse: 5′-CTCAACACGAGGTCTTGGTGCA-3′.

2.8 Immunoprecipitation and Immunoblotting Analysis

Protein A agarose beads (Millipore, Billerica, MA, USA) were washed three times with PBS before the addition of anti-GFP antibody. This mixture was incubated for 3 hours at 4 °C. Protein was extracted from HEK-293T cells using the following lysis buffer: 50 mM Tris–HCl pH 7.5, 0.1% SDS, 1% TritonX-100, 150 mM NaCl, 1 mM dithiothreitol, 0.5 mM EDTA, 100 mM PMSF, 100 mM leupeptin, 1 mM aprotinin, 100 mM sodium orthovanadate, 100 mM sodium pyrophosphate, and 1 mM sodium fluoride. Cell extracts were centrifuged at 13,000 g for 10 min and the resulting supernatants were added to the bead and antibody mixture. Following overnight incubation at 4 °C, the immunocomplexes were washed three times with lysis buffer and then subjected to immunoblotting using specific antibodies. Image Lab software (Bio-Rad, version 3.0, Berkeley, CA, USA) was used to quantify the band intensity.

2.9 Immunofluorescence

Approximately 3000 cells were seeded into a 24-well plate and grown for 24 hours at 37 °C. The cells were then fixed with 4% paraformaldehyde (Sigma) for 10 min, followed by permeabilization with 0.1% Triton X-100 (Sigma) for 10 minutes and then blocking with 10% bovine serum albumin (BSA) (Sigma) at room temperature for 1 hour. The primary antibodies anti-GFP, anti-PDHK1 and anti-PDHA1 were diluted (1:100) in 2% BSA and 20 µL was added to each sample and incubated overnight. After washing, secondary antibodies diluted with 2% BSA and mixed with DAPI were added to each sample and incubated for 1 h. The cells were then viewed using a Leica TCS SP8 confocal microscope.

2.10 Immunohistochemistry

Sections of bladder tissue on slides were purchased from Shuangxuan company (Wuhan, China). The slides were deparaffinized by immersing twice in xylene for 5 minutes each, and then immersed twice in 100% alcohol for 3 minutes each. This was followed by sequential immersion in 95%, 85%, and 75% alcohol for 3 minutes each. Antigen retrieval was achieved by boiling the slide in citric acid (pH = 6.0) for 20 minutes, then cooling to room temperature. Endogenous peroxidase activity was blocked by incubating the sections in a 3% H_2O_2 solution (ZSGB-BIO, Beijing, China) in methanol at room temperature for 10 minutes. The tissue was then blocked with 5% BSA for 1 hour, followed by the addition of 50 µL anti-*PPP3CB* antibody and overnight incubation at 4 °C. Subsequently, Sav-HRP (ZSGB-BIO) conjugates were applied to the sections and incubated at room temperature for 30 minutes. This was followed by the addition of 50 µL DAB substrate solution

(ZSGB-BIO) to the sections for approximately 1 minute to visualize the antibody staining. Tissue slides were then dehydrated by sequential immersion in alcohol solutions (85%, 98%, 100%, 100%) for 5 minutes each, with the process repeated four times. This was followed by immersion in xylene three times. A microscope was used to visualize the antibody staining in the tissue sections.

2.11 Glucose Uptake and Lactate Production Assays

Extracellular lactate and glucose concentrations were quantified under normoxic conditions using lactate (solarbio, BC2230, Beijing, China) and glucose (solarbio, BC2505) assay kits, respectively. Briefly, 1×10^6 cells suspended in 2 mL of medium were seeded into 6-well dishes. After 6 hours, the medium was replaced with serum-free DMEM. For the assessment of glucose consumption and lactate production, cells were incubated for 18 hours and 8 hours, respectively. The culture supernatant was then collected to measure the concentrations of glucose and lactate as described by the manufacturer of each kit.

The measurement of glucose content involved three reagents within the kit. Use as described by the manufacturer of each kit.

2.12 In Vivo Xenograft Experiment

The animal studies conducted in this research were approved by the Animal Research Ethics Committee of Chongqing Medical University. Male BALB/c mice aged 6-weeks were housed and maintained in the experimental animal center of Chongqing Medical University. A total of 4×10^6 cells with or without *PPP3CB* knockout were resuspended in 100 µL of PBS and subcutaneously injected into the hind leg flanks of the mice. Tumor growth was monitored every three days after inoculation by measuring the width (W) and height (H) of the tumor. The tumor volume (V) was calculated using the formula: V = (H × W^2) / 2. All mice were euthanized 5 weeks after cell injection and the tumor was harvested and its weight measured.

2.13 Flow Cytometry

A total of 5×10^5 T24 cells were seeded into 6-well dishes and incubated for 48 hours. The cells were then washed three times with PBS and digested using EDTA-free trypsin. Subsequently, the cells were centrifuged at 2500 rpm for 5 minutes and the supernatant discarded. The cell pellet was resuspended in 1 ml of PBS and analyzed by flow cytometry for the detection of apoptosis.

2.14 Metabolomic Analysis

T24 cells were digested and centrifuged at 1000 rpm, washed three times with PBS, snap frozen with liquid nitrogen and then stored at –80 °C. Untargeted metabolomics were performed using Ultra High Performance Liquid Chromatography (UHPLC) (1290 Infinity II, Agilent Technologies, Santa Clara, CA, USA) equipped with a quadrupole time-of-flight mass spectrometer (AB Sciex TripleTOF 6600) at Shanghai Applied Protein Technology Co., Ltd. (Shanghai, China). Cell metabolites were separated on an ACQUITY UHPLC BEH Amide column under optimized conditions. The samples were kept at 4 °C throughout the UHPLC-Mass Spectrometry (UHPLC-MS) analysis. Mass spectrum analysis was performed using the electrospray ionization (ESI) source in both positive and negative modes. Metabolite identification was carried out by converting the raw MS data to mzXML files and analyzing with XCMS software (Mass Consortium, version 4.0.0, La Jolla, CA, USA). Metabolites were identified by comparing their m/z values and MS/MS spectra with an in-house database of authentic standards and metabolic reaction network. All metabolomic sample readings were averaged.

2.15 Statistical Analysis

Statistical analysis was performed using Graphpad Prism 8 software (GraphPad Software Inc., La Jolla, CA, USA). * $p < 0.05$, ** $p < 0.01$, *** $p < 0.001$, and **** $p < 0.0001$ denoted statistically significant differences compared with the control group. Two-sided Student's *t*-tests were performed for two-group comparisons.

3. Results

3.1 PPP3CB is Downregulated in Bladder Cancer

PPP3CB was recently reported to be a key regulator of epithelial-mesenchymal transition (EMT) in G401 cells [15]. However, the function of *PPP3CB* in bladder cancer remains unclear. Bioinformatic analysis of the TCGA cohort revealed that *PPP3CB* is significantly downregulated in bladder tumor tissue (Fig. 1A,B). To confirm this result, we performed immunohistochemical (IHC) staining of bladder cancer tissue using tissue microarrays. This revealed that most tumor tissues have lower *PPP3CB* expression levels compared with their paired normal tissue (Fig. 1C,D), indicating that *PPP3CB* is a potential suppressor in bladder cancer.

3.2 PPP3CB Promotes Apoptosis and Inhibits the Proliferation of Bladder Cancer Cells

In order to validate the anti-tumor effect of *PPP3CB in vitro*, we performed *PPP3CB* overexpression and knockout experiments in T24 cells. Flow cytometry showed that overexpression of *PPP3CB* promotes the apoptosis of T24 cells (Fig. 2A–C). In contrast, knockout of *PPP3CB* inhibited the apoptosis of T24 cells. We also investigated the effect of *PPP3CB* on the proliferation of T24 cells (Fig. 2D–F). Cell viability assays revealed that *PPP3CB* overexpression inhibited the growth of T24 cells (Fig. 2G), whereas knockout of *PPP3CB* promoted their proliferation (Fig. 2J). Consistent with these findings, the colony formation assay revealed that *PPP3CB* overexpression suppressed the colony formation ability of T24 cells

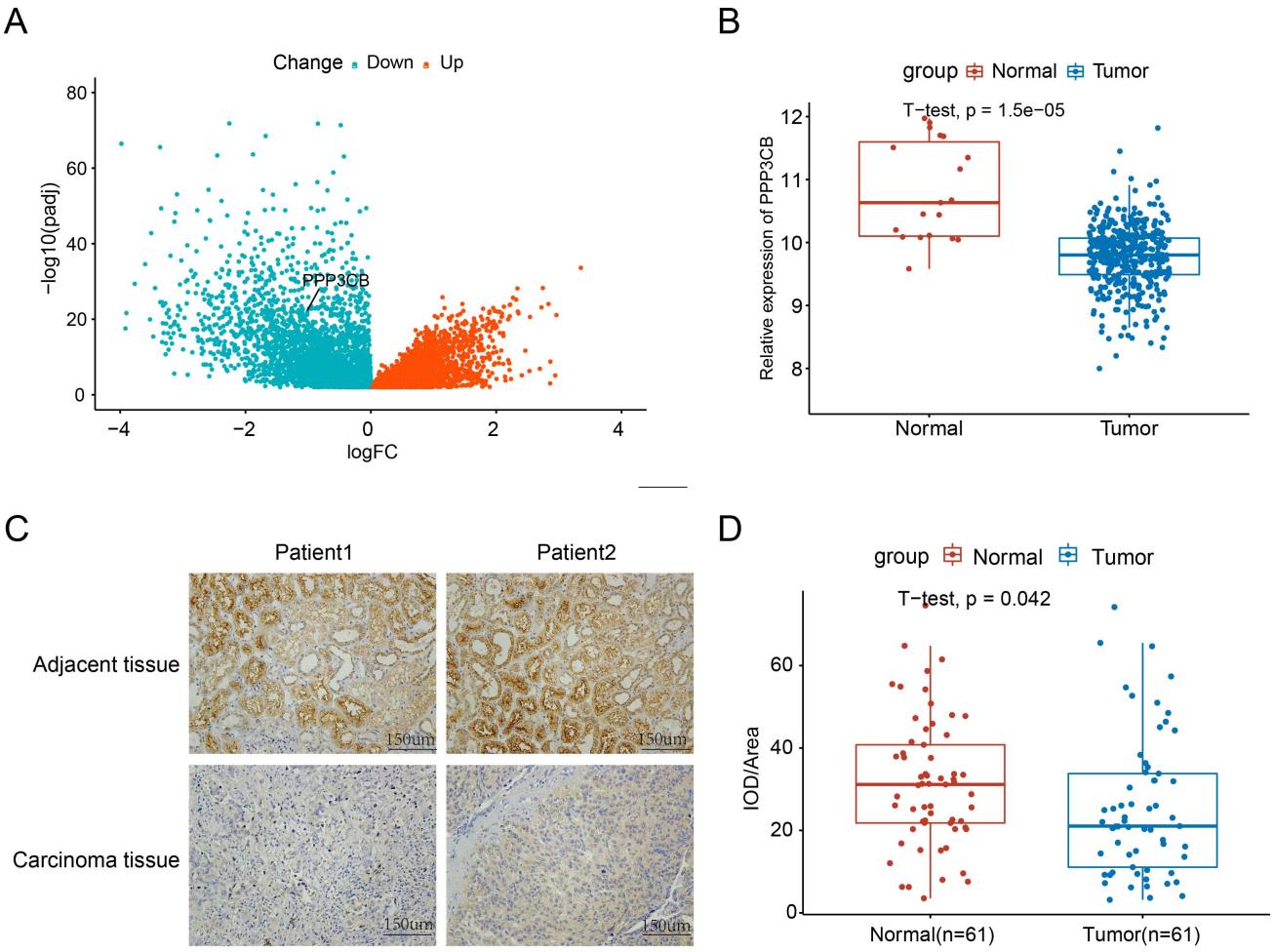

Fig. 1. *PPP3CB* expression is downregulated in bladder cancer. (A) *PPP3CB* expression in bladder cancer is low in the The Cancer Genome Atlas (TCGA) cohort. (B) The *PPP3CB* expression level in bladder cancer tissue was significantly lower than in para-cancerous tissue. (C) Immunohistochemical (IHC) staining showing lower *PPP3CB* expression in the tumor tissue of bladder cancer patients compared to adjacent normal tissue. (D) Average integrated optical density (IOD) in bladder cancer tissue was lower than in adjacent tissue. Error bars represent the mean ± standard deviation (SD) of three experimental replicates. Statistical significance was assessed using a two-tailed unpaired Student's *t*-test.

(Fig. 2H,I), whereas knockout of *PPP3CB* promoted colony formation (Fig. 2K,L). Collectively, these results suggest that *PPP3CB* can inhibit the proliferation of bladder cancer cells *in vitro* and promote their apoptosis.

3.3 PPP3CB Inhibits Glycolysis in Bladder Cancer Cells

To investigate whether *PPP3CB* deficiency promotes the proliferation of T24 cells through glucose metabolism, we first examined glucose metabolism after knockdown of *PPP3CB*. Specifically, metabolomics was performed to investigate differences in intracellular metabolites between the negative control and *PPP3CB* knockdown cells (Fig. 3A). The increase in glycolysis metabolites after *PPP3CB* knockdown (Fig. 3B) indicates a pivotal role for *PPP3CB* in T24 cell glucose metabolism. To confirm these results, we also measured glucose uptake and lactate production. Consistent with the above findings, overexpression of *PPP3CB* reduced glucose uptake and lactose production (Fig. 3C,D), whereas knockdown of *PPP3CB* increased glucose uptake and lactate production (Fig. 3E,F). Collectively, these results suggest that *PPP3CB* is a negative regulator of glucose metabolism in T24 cells.

3.4 PPP3CB Downregulates PDHK1 Expression

Due to the upregulation of lactate, we deduced that *PPP3CB* may affect the expression of LDHA. However, the results showed no difference in LDHA level between the two groups (**Supplementary Fig. 1**). Therefore, we next examined whether the change in glucose metabolism could be attributed to changes in pyruvate dehydrogenase (PDH). For this, we evaluated the expression levels of pyruvate dehydrogenase E1 subunit alpha1 (PDHA1), phospho-PDHA1, pyruvate dehydrogenase E1 subunit beta (PDHB), and pyruvate dehydrogenase kinase 1 (PDHK1). Interest-

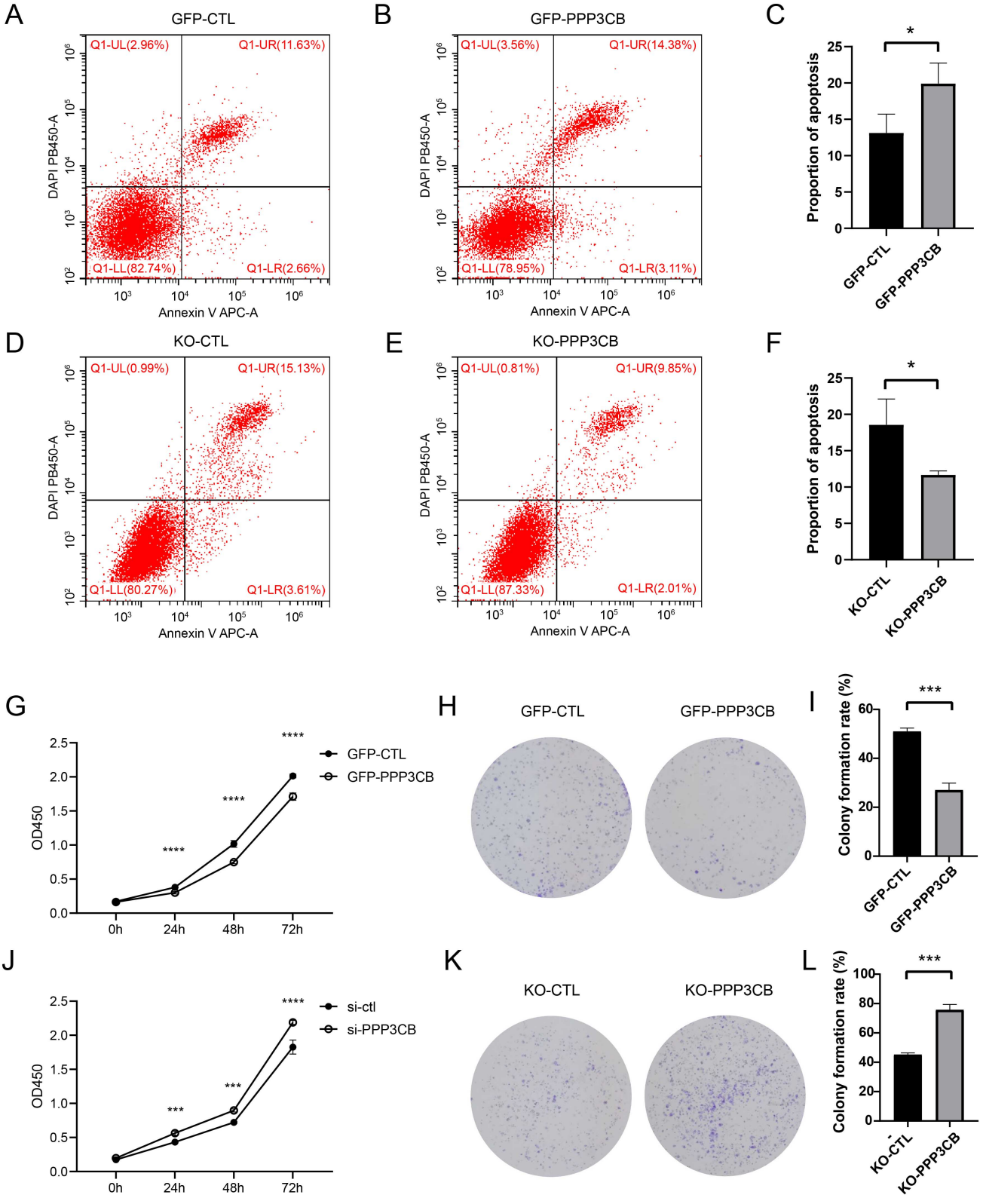

Fig. 2. *PPP3CB* inhibits the proliferation of bladder cancer cells and promotes their apoptosis. (A–C) *PPP3CB* overexpression promotes the apoptosis of T24 cells. (D–F) Knockout of *PPP3CB* inhibits the apoptosis of T24 cells. (G) *PPP3CB* overexpression inhibits the proliferation of T24 cells. (H,I) Overexpression of *PPP3CB* inhibits colony formation of T24 cells. (J) Knockout of *PPP3CB* promotes the proliferation of T24 cells. (K,L) Knockout of *PPP3CB* promotes colony formation by T24 cells. Error bars represent the mean ± SD of three replicate experiments. Statistical significance was assessed using a two-tailed unpaired Student's *t*-test. *$p < 0.05$, ***$p < 0.001$, ****$p < 0.0001$.

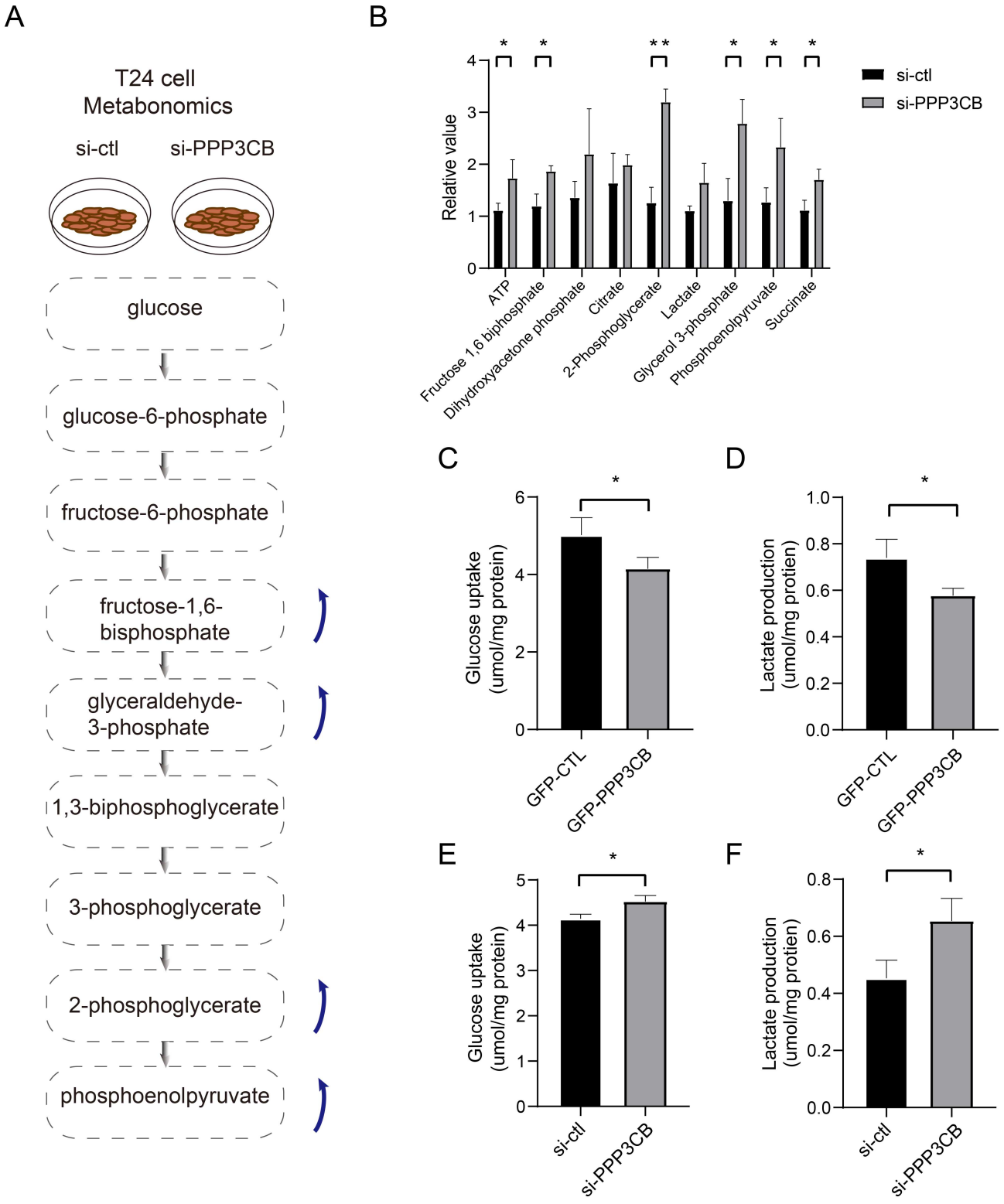

Fig. 3. *PPP3CB* inhibits glycolysis in bladder cancer cells. (A) Schematic representation of the metabolic pathways and specific metabolites affected by *PPP3CB* knockout in T24 cells. (B) Knockdown of *PPP3CB* upregulates glycolysis intermediates. (C,D) Over-expression of *PPP3CB* decreases glucose uptake and lactate production. (E,F) Knockdown of *PPP3CB* enhances glucose uptake and lactate production. Error bars represent the mean ± SD of three experimental replicates. Statistical significance was assessed using a two-tailed unpaired Student's *t*-test, *$p < 0.05$, **$p < 0.01$.

ingly, knockdown of *PPP3CB* in T24 cells resulted in increased expression levels of PDHK1 and p-PDHA1, but not PDHB or PDHA1 (Fig. 4A, **Supplementary Fig. 3**). In line with this, knockout of *PPP3CB* also increased the expression of PDHK1 and p-PDHA1 (Fig. 4B,C). In contrast, the overexpression of *PPP3CB* in T24 cells led to a reduction in the expression of PDHK1 and p-PDHA1 (Fig. 4D,E). We next investigated whether increased expression of PDHK1 was due to changes in mRNA or protein stability. Quantitative real-time PCR showed the mRNA level increased after knockdown of *PPP3CB* (**Supplementary Fig. 2**). Knockdown of *PPP3CB* also attenuated the degradation of PDHK1 after cycloheximide (CHX) treatment (Fig. 4F,G). These results indicate that knockdown of *PPP3CB* enhances PDHK1 protein expression by increasing its transcription level and stabilizing protein expression.

3.5 PPP3CB Interacts with the Catalytic Domain of PDHK1

To further study the mechanism by which PDHK1 expression increased, immunofluorescence (IF) was performed to evaluate the co-localization of *PPP3CB* and PDHK1, while co-immunoprecipitation (co-IP) was used to examine the interaction between these proteins. IF showed that *PPP3CB* co-localized with PDHK1 in T24 cells (Fig. 5A). Exogenous PDHK1 was also found to interact with endogenous *PPP3CB* in T24 cells (Fig. 5B). Moreover, exogenous PDHK1 interacted with both exogenous *PPP3CB* (Fig. 5C) and endogenous *PPP3CB* (Fig. 5D) in HEK-293T. In line with this, co-IP revealed that exogenous *PPP3CB* interacted with exogenous PDHK1 in HEK-293T (Fig. 5E). To identify the precise interaction domain of *PPP3CB*, we constructed plasmids with different deletion mutations of *PPP3CB* (Fig. 5F). co-IP experiments with HEK-293T cells showed that *PPP3CB* interacted with the PDHK1 catalytic domain and with the calcineurin B binding domain (Fig. 5G).

Taken together, these results indicate that *PPP3CB* interacts with PDHK1, resulting in the destabilization and degradation of PDHK1. Hence, the low expression of *PPP3CB* in bladder cancer cells leads to reduced degradation of PDHK1, thereby promoting the Warburg effect.

3.6 DCA Inhibits Glycolysis and the Proliferation of Bladder Cancer Cells

Since *PPP3CB* interacts with PDHK1, we inferred that *PPP3CB* inhibits glycolysis and the proliferation of bladder cancer cells through PDHK1. We therefore treated T24 cells with DCA, which is an inhibitor of PDHK1 [24]. Both PDHK1 and p-PDHA1 expression were significantly downregulated by DCA (Fig. 6A), with flow cytometry also showing increased apoptosis (Fig. 6B–D). In line with this, the cell viability and colony formation assays showed that proliferation of T24 cells was suppressed by DCA (Fig. 6E–G). Furthermore, treatment with DCA inhibited glucose uptake and lactate production in T24 cells (Fig. 6H,I). As stated previously, overactivated PDHK1 can inhibit PDC, thereby switching tumor cells from oxidative phosphorylation to glycolysis and promoting bladder cancer cell proliferation. The present results confirm that inhibition of PDHK1 with DCA blocks glycolysis and the proliferation of bladder cancer cells.

3.7 PPP3CB Inhibits Glycolysis and the Proliferation of Bladder Cancer Cells by Targeting PDHK1

In order to confirm that increased glycolysis and cell proliferation induced by *PPP3CB* knockdown were due to PDHK1, we conducted immunoblot analysis to determine the expression level of p-PDHA1 in T24 cells. DCA was used to inhibit PDHK1 due to its relative specificity for this enzyme. The upregulation of p-PDHA1 after *PPP3CB* knockdown was found to be blocked by DCA treatment (Fig. 7A, **Supplementary Fig. 4**). This indicates that *PPP3CB* upregulates the expression of both PDHK1 and p-PDHA1, whereas DCA treatment reversed this effect. Next, flow cytometry revealed that DCA could block apoptosis resulting from *PPP3CB* knockdown (Fig. 7B–E). In line with this, the proliferation of T24 cells after *PPP3CB* knockout was attenuated by DCA treatment (Fig. 7F–H). As expected, glucose uptake and lactate production were significantly upregulated after *PPP3CB* knockdown, but DCA treatment blocked this effect (Fig. 7I,J). Nevertheless, our findings indicate that *PPP3CB* deficiency increases glycolysis and the proliferation of T24 cells by upregulating the expression of PDHK1.

3.8 Depletion of PPP3CB Promotes Bladder Cancer Growth in Vivo

To investigate the tumor-promoting effect of *PPP3CB* deficiency, we established a xenograft mouse model by injecting T24 cells with or without *PPP3CB* knockout (Fig. 8A, **Supplementary Fig. 5**). The results showed that injection of T24 cells with *PPP3CB* knockout resulted in significantly higher tumor weight and volume in nude mice (Fig. 8B,C), thus demonstrating the anti-tumor effect of *PPP3CB in vivo*.

As shown in Fig. 9, deficiency of *PPP3CB* stabilizes PDHK1, thereby increasing phospho-PDHA1. This deactivates the PDC, leading to an enhanced Warburg effect and faster growth of bladder tumors.

4. Discussion

The reprogramming of glucose metabolism in cancer cells towards “aerobic glycolysis” has received considerable attention in the scientific community, with the “Warburg effect” recognized as one of the established hallmarks of cancer [25]. Unlike most normal cells that metabolize glucose to carbon dioxide instead of lactate, tumor cells produce large amounts of lactate independently of oxygen supply [26]. This metabolic switch is regulated by oncogenes

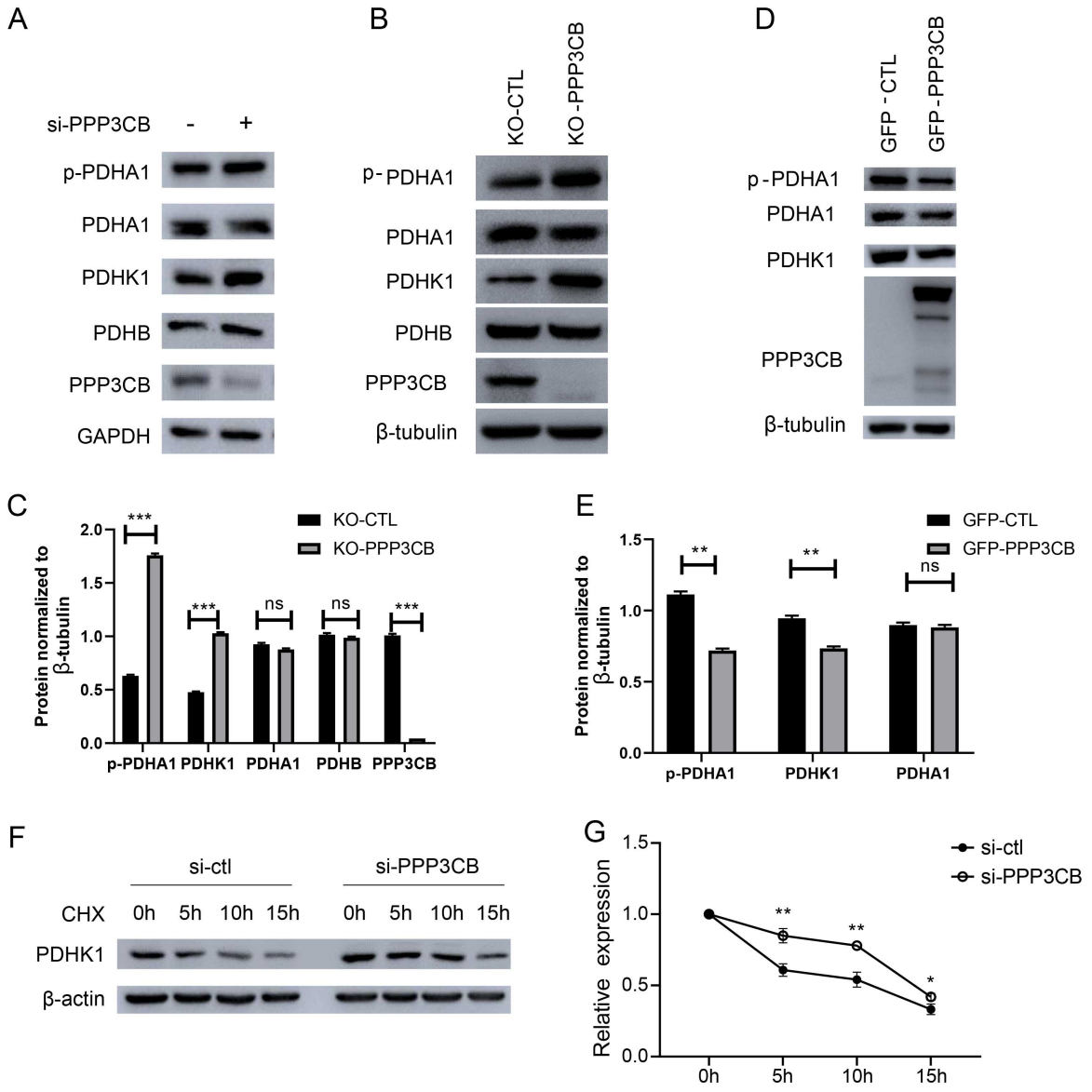

Fig. 4. *PPP3CB* decreases the expression pyruvate dehydrogenase kinase 1 (PDHK1). (A) Knockdown of *PPP3CB* increased the expression of PDHK1 in normoxia and in $CoCl_2$-induced hypoxia. (B) Knockout of *PPP3CB* increased the expression of PDHK1. (C) Protein quantification after knockout of *PPP3CB*. The results shown are the mean ± SEM (n = 3). NS, not significant; ***$p < 0.001$. (D) Overexpression of *PPP3CB* reduced the expression of PDHK1. (E) Protein quantification following the overexpression of *PPP3CB*. The results shown are the mean ± standard error of the mean (SEM) (n = 3). NS, not significant; **$p < 0.01$. (F,G) Knockdown of *PPP3CB* enhanced the stability of PDHK1. *$p < 0.05$, **$p < 0.01$.

and tumor suppressor genes and enables the high rate of proliferation and division of tumor cells [27]. Bladder cancers also exhibit high lactate production and downregulation of pyruvic acid [8]. Many biomarkers have been associated with glucose metabolism in bladder cancer. Cao *et al.* [28] reported that ROCR regulates cell proliferation, glucose metabolism and chemoresistance in bladder cancer, specifically through its involvement in the PD-L1/ITGB6/STAT3 signaling axis. In addition, Wang *et al.* [29] highlighted the pivotal role of the HIF-1α/ALYREF/PKM2 axis in glycolysis and proliferation in bladder cancer.

Protein phosphatase 2B (PP2B) can act on a large cross-section of protein substrates in response to intracellular calcium [30]. Recent research has revealed that PP2B plays a vital role in cancer. Chen *et al.* [31] reported that PP2B dephosphorylates c-Jun in A431 cells to regulate c-Jun/Sp1 interactions. As one of the catalytic subunits of PP2B, *PPP3CB* has been reported to inhibit the migration of G401 cells [15]. Furthermore, suppression of *PPP3CB* transcription leads to Herceptin resistance in HER2-positive breast cancer [32]. These studies provide novel insights into the role of *PPP3CB* in cancer. *PPP3CB*

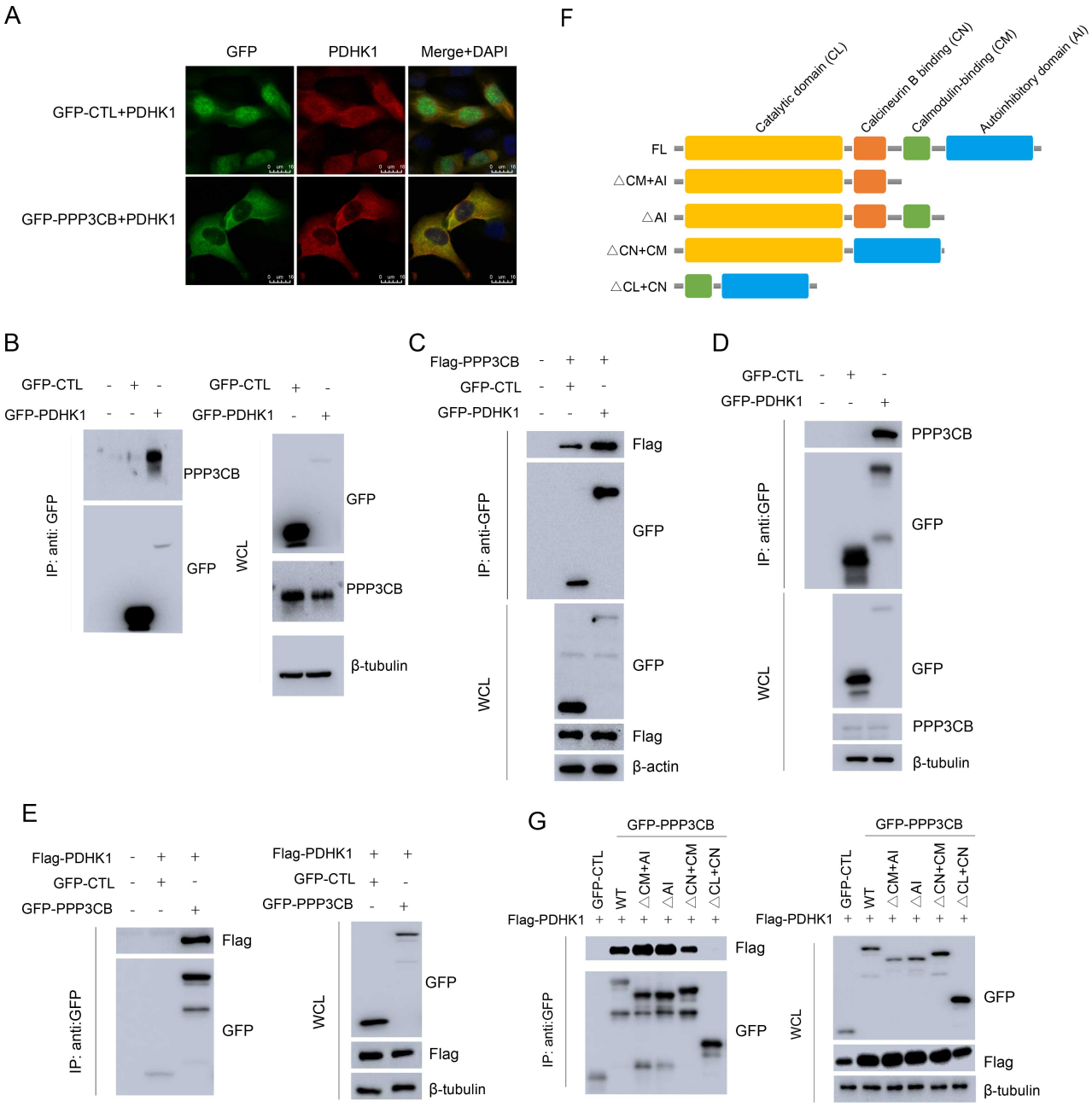

Fig. 5. *PPP3CB* interacts with PDHK1. (A) Immunofluorescence showing the co-localization of *PPP3CB* with PDHK1 in T24 cells. (B) GFP-PDHK1 interacting with endogenous *PPP3CB* in T24 cells. (C) GFP-PDHK1 interacting with Flag-*PPP3CB* in HEK-293T cells. (D) GFP-PDHK1 interacting with endogenous *PPP3CB* in HEK-293T cells. (E) GFP-*PPP3CB* interacting with Flag-PDHK1 in HEK-293T cells. (F) The structural domain of *PPP3CB*. (G) *PPP3CB* mainly interacts with the catalytic domain of PDHK1 in HEK-293T cells.

is also involved with metabolism. Pfluger *et al.* [14] reported that *PPP3CB* deficiency increases mitochondrial elongation and respiration, and protects mice from diet-induced obesity, thus indicating its critical function in lipid metabolism. Although Vasu *et al.* [33] reported that hyperglycemia could elevate the mRNA expression level of *PPP3CB* in a human pancreatic β-cell line, there is no evidence that *PPP3CB* can regulate glucose metabolism in normal or malignant human cells. It is therefore important to determine whether *PPP3CB* is involved in the glucose metabolism of cancer cells, and to elucidate the association between *PPP3CB*-regulated cell proliferation and glucose metabolism.

Here, we studied the potential involvement of *PPP3CB* in the glucose metabolism and cell proliferation of bladder cancer. Based on the TCGA database and the analysis of human tissues, our findings indicate that *PPP3CB* expression is significantly lower in bladder cancer than

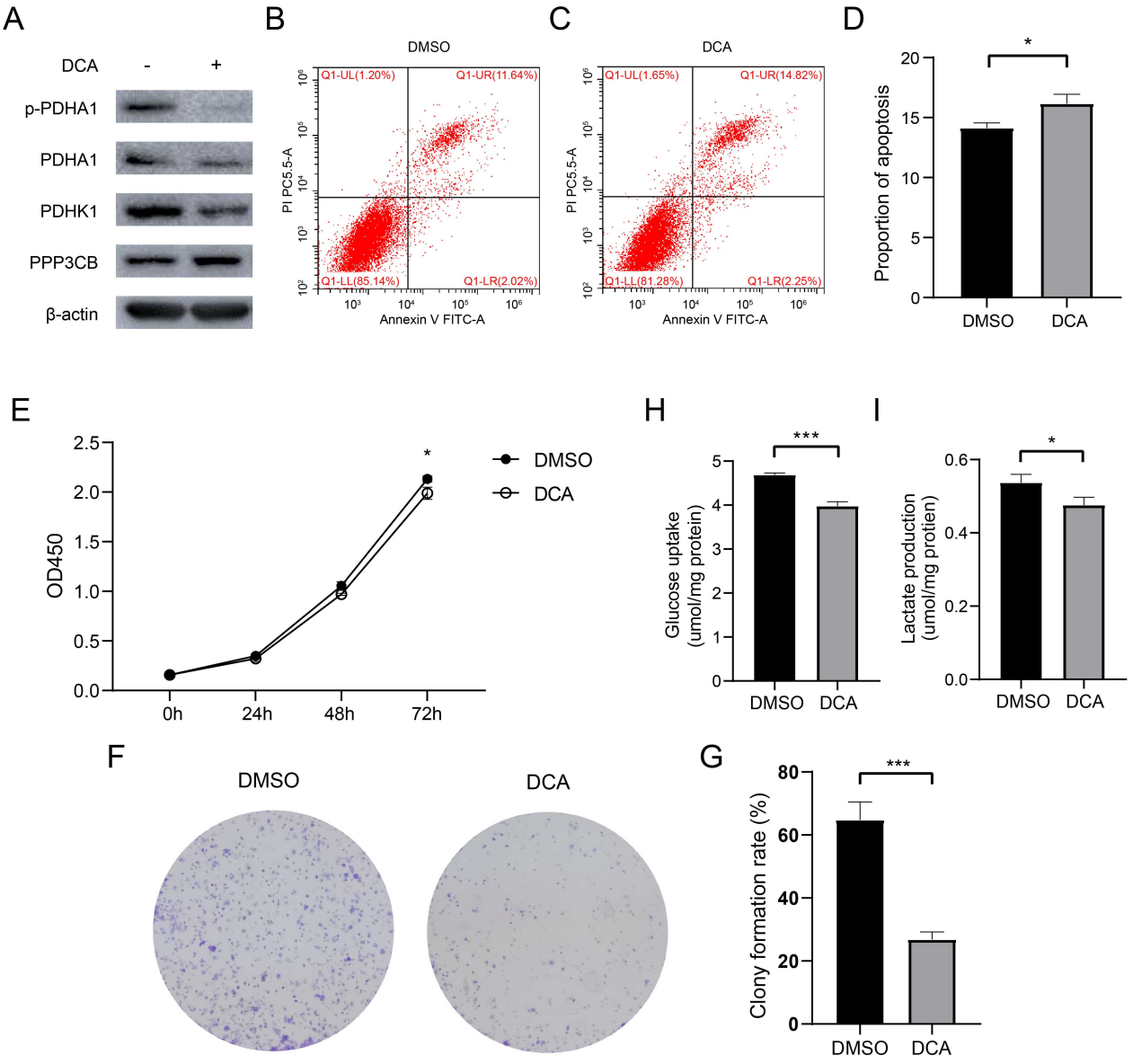

Fig. 6. Dichloroacetate (DCA) promotes apoptosis and inhibits proliferation and glycolysis in T24 cells. (A) Suppression of PDHA1 phosphorylation by DCA treatment of T24 cells for 2 hours. (B–D) DCA treatment increases apoptosis. (E) DCA treatment inhibits the proliferation of T24 cells. (F,G) Decreased colony number after DCA treatment. For the Cell Counting Kit-8 (CCK-8) and clonal formation assays, DCA was added 24 hours after cell seeding. (H,I) DCA treatment (0.5 mmol/L) decreased glucose uptake and lactate production. *$p < 0.05$, ***$p < 0.001$.

in paracancerous tissues. This result was verified by *in vitro* experiments showing that *PPP3CB* inhibited the proliferation of bladder cancer cells and induced their apoptosis. Subsequently, non-targeted metabolomic analysis of T24 cells revealed that *PPP3CB* knockdown can upregulate sugar metabolites. In a similar manner, knockdown of *PPP3CB* in bladder cancer cells resulted in increased lactate production and glucose uptake, whereas overexpression of *PPP3CB* had the opposite effect. These findings indicate that *PPP3CB* is involved in the regulation of glycolysis in T24 cells. Since the level of LDHA did not change following *PPP3CB* knockdown, we assessed the protein expression levels within the PDC, with a particular focus on PDHK1. PDHK1 has been reported to impair $CD8^+$ T cell function in ovarian cancer cells by upregulating PD-L1 [34]. Fujiwara *et al.* [35] suggested that inhibition of PDHK1 may be a novel therapeutic approach for multiple myeloma. PDHK1 has also been identified as a potential biomarker for bladder cancer [36], although the upstream mechanism that underlies its effect on proliferation is still unclear. Other work has shown that p-PDHA1 is upregulated after *PPP3CB* knockdown, indicating impaired PDH activity [37]. This finding was confirmed by the overexpression of *PPP3CB*, which could therefore explain the ac-

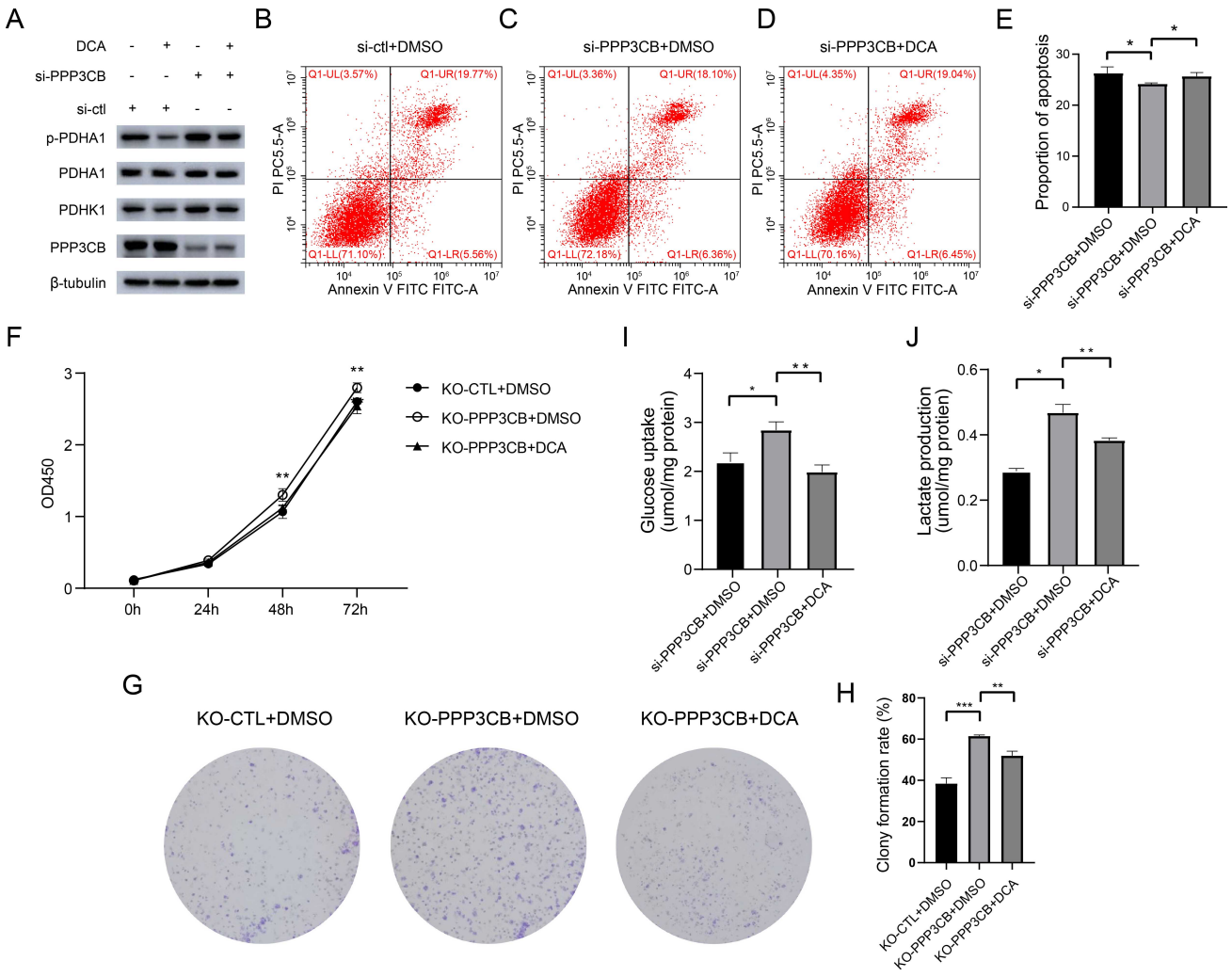

Fig. 7. *PPP3CB* knockdown promotes cell proliferation and inhibits apoptosis by upregulating PDHK1. (A) DCA blocks the upregulation of PDHK1 after *PPP3CB* knockdown in T24 cells. (B–E) DCA abolishes the effect of *PPP3CB* knockdown on apoptosis. (F) DCA blocks the increased proliferation of T24 cells after *PPP3CB* knockout. Statistical analysis was performed using a two-way ANOVA with Bonferroni's post hoc test. (G,H) DCA abolishes the increased number of T24 cell colonies induced by *PPP3CB* knockout. (I,J) DCA blocks the increase in glucose uptake and lactate production induced by *PPP3CB* knockdown. $*p < 0.05$, $**p < 0.01$, $***p < 0.001$.

tivated glycolysis. The present study revealed the increase in PDHK1 expression observed after *PPP3CB* knockdown was due to greater protein stability. Additionally, co-IP experiments revealed the *PPP3CB* catalytic domain could interact with PDHK1. Although we cannot exclude the possibility of a transcriptional effect of *PPP3CB* on PDHK1, we speculate involvement of the ubiquitin-proteasome degradation pathway. *PPP3CB* could dephosphorylate the E3 ligase of PDHK1, thereby promoting its degradation. In any case, further studies will be required to explain the high stability of PDHK1 in bladder cancer cells that express low levels of *PPP3CB*.

We therefore propose that increased glycolysis and enhanced proliferation in cells with *PPP3CB* knockdown are due to elevated PDHK1 expression. DCA, an inhibitor of PDHK1, maintains PDC in an unphosphorylated and active state, thereby reversing the Warburg effect in tumor cells [38]. The present study found that DCA treatment significantly downregulated p-PDHA1 expression. In addition, apoptosis was promoted and proliferation was inhibited in bladder cancer cells treated with DCA, consistent with the results of a previous study [39]. As expected, DCA treatment inhibited glucose uptake and lactate production. Furthermore, we found that DCA treatment reversed the effects of *PPP3CB* knockdown, i.e., increased cell proliferation, reduced apoptosis and increased glycolysis. These results demonstrate that *PPP3CB* regulates proliferation and glycolysis in bladder cancer cells through PDHK1. Finally, our *in vivo* experiments confirmed the pro-tumor effect of *PPP3CB* deficiency. A limitation of this study is that the underlying mechanism for the increased PDHK1 stability after *PPP3CB* knockdown is still unclear and requires fur-

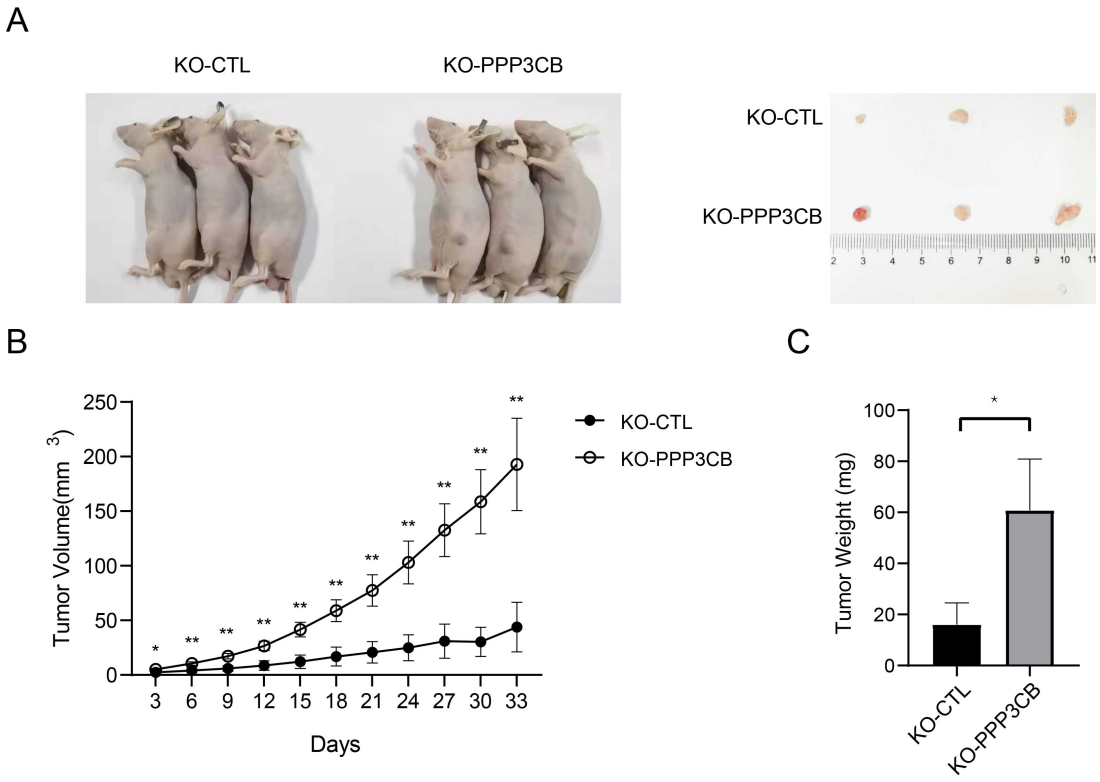

Fig. 8. Knockout of *PPP3CB* promotes the growth of bladder tumors formed by injection of T24 cells. (A) Sacrificed mice and the corresponding tumors. (B) Greater tumor volume in *PPP3CB* knockout tumors. (C) Increased tumor weight of *PPP3CB* knockout tumors. Error bars represent the mean ± SD of three experimental replicates. Statistical significance was assessed using a two-tailed unpaired Student's *t*-test. $*p < 0.05$, $**p < 0.01$.

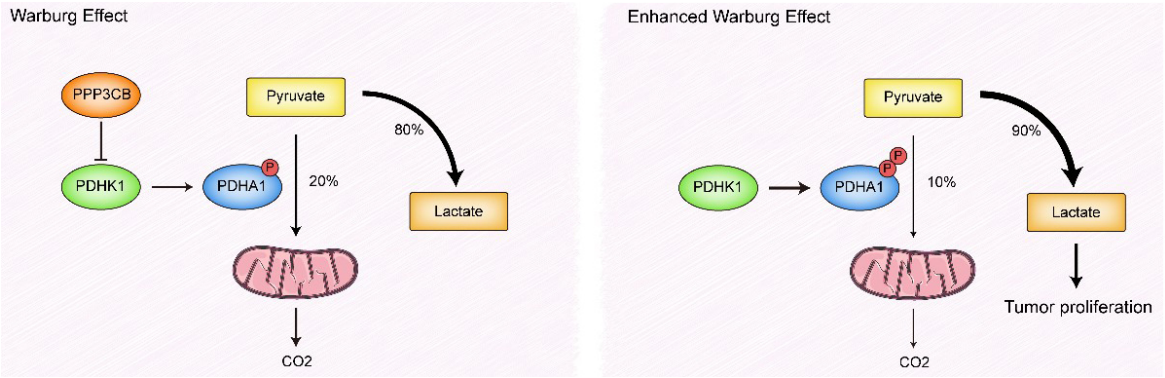

Fig. 9. Working model derived from the study results. P represents phosphorylation of PDHA1.

ther in-depth investigation. Whether other molecular mechanisms are involved in the degradation of PDHK1 also requires additional study.

5. Conclusions

The summary of our findings and conclusions are shown in Fig. 9. A range of tumorigenic factors have been shown to induce PDC dysfunction in bladder cancer cells. This results in the majority of pyruvate being directed towards anaerobic metabolism to produce lactate, rather than CO_2 in the mitochondria. PDHK1 expression was found here to be upregulated in *PPP3CB*-deficient bladder cancer cells, thereby facilitating the phosphorylation of PDHA1 and leading to inactivation of PDC and accumulation of lactic acid. *PPP3CB* deficiency therefore exacerbates the Warburg effect and increases the proliferation of bladder cancer cells. This study expands our understanding of the regulatory mechanism involving pyruvate dehydrogenase, and suggests that targeting of *PPP3CB* may be a potentially effective therapeutic strategy for bladder cancer.

Availability of Data and Materials

The datasets used and/or analyzed during the current study are available from the corresponding author on reasonable request.

Author Contributions

All authors have participated sufficiently in the work and agreed to be accountable for all aspects of the work. QL and TS designed the project, XQ and ZJ performed the experiments, XQ wrote the manuscript, YL interpret part of data for the work, DT analyzed the data. All authors contributed to the revision of this manuscript and approved the final manuscript.

Ethics Approval and Consent to Participate

The Ethics Committee of Chongqing Medical University has reviewed the proposed use of human subjects in the projects. It is recognized that the rights and the welfare of the subjects are adequately protected; the potential risks are outweighed by potential benefits. The species, strains, grade, specification and number of the animals to be used are justified. Appropriate animal care throughout the experiment, including anesthetics, sedatives should be used. Disposition of animals at the end of study euthanasia criteria and method is in accordance with the code of practice for the care and use of animals for scientific purposes.

Acknowledgment

Not applicable.

Funding

This work was supported by (1) Chongqing Natural Science Foundation project (NO. cstc2021jcyj-msmX0019). (2) Project Supported by Scientific and Technological Research Program of Chongqing Municipal Education Commission (NO. KJQN202000438). (3) Chongqing Municipal Key Project for Technological Innovation and Application Development (NO. cstc2019jscx-dxwtBX0032).

Conflict of Interest

The authors declare no conflict of interest.

Supplementary Material

Supplementary material associated with this article can be found, in the online version, at https://doi.org/10.31083/j.fbl2902048.

References

[1] Bray F, Ferlay J, Soerjomataram I, Siegel RL, Torre LA, Jemal A. Global cancer statistics 2018: GLOBOCAN estimates of incidence and mortality worldwide for 36 cancers in 185 countries. CA: a Cancer Journal for Clinicians. 2018; 68: 394–424.

[2] Lenis AT, Lec PM, Chamie K, Mshs MD. Bladder Cancer: A Review. JAMA. 2020; 324: 1980–1991.

[3] Hay N. Reprogramming glucose metabolism in cancer: can it be exploited for cancer therapy? Nature Reviews. Cancer. 2016; 16: 635–649.

[4] WARBURG O. On the origin of cancer cells. Science (New York, N.Y.). 1956; 123: 309–314.

[5] Massari F, Ciccarese C, Santoni M, Iacovelli R, Mazzucchelli R, Piva F, *et al*. Metabolic phenotype of bladder cancer. Cancer Treatment Reviews. 2016; 45: 46–57.

[6] Hoskin PJ, Sibtain A, Daley FM, Wilson GD. GLUT1 and CAIX as intrinsic markers of hypoxia in bladder cancer: relationship with vascularity and proliferation as predictors of outcome of ARCON. British Journal of Cancer. 2003; 89: 1290–1297.

[7] Al Hasawi N, Alkandari MF, Luqmani YA. Phosphofructokinase: a mediator of glycolytic flux in cancer progression. Critical Reviews in Oncology/Hematology. 2014; 92: 312–321.

[8] Dettmer K, Vogl FC, Ritter AP, Zhu W, Nürnberger N, Kreutz M, *et al*. Distinct metabolic differences between various human cancer and primary cells. Electrophoresis. 2013; 34: 2836–2847.

[9] Conde VR, Oliveira PF, Nunes AR, Rocha CS, Ramalhosa E, Pereira JA, *et al*. The progression from a lower to a higher invasive stage of bladder cancer is associated with severe alterations in glucose and pyruvate metabolism. Experimental Cell Research. 2015; 335: 91–98.

[10] Lea MA, Altayyar M, desBordes C. Inhibition of Growth of Bladder Cancer Cells by 3-(3-Pyridinyl)-1-(4-pyridinyl)-2-propen-1-one in Combination with Other Compounds Affecting Glucose Metabolism. Anticancer Research. 2015; 35: 5889–5899.

[11] Zhao W, Chang C, Cui Y, Zhao X, Yang J, Shen L, *et al*. Steroid receptor coactivator-3 regulates glucose metabolism in bladder cancer cells through coactivation of hypoxia inducible factor 1α. The Journal of Biological Chemistry. 2014; 289: 11219–11229.

[12] Langbein S, Zerilli M, Zur Hausen A, Staiger W, Rensch-Boschert K, Lukan N, *et al*. Expression of transketolase TKTL1 predicts colon and urothelial cancer patient survival: Warburg effect reinterpreted. British Journal of Cancer. 2006; 94: 578–585.

[13] Shakhova I, Li Y, Yu F, Kaneko Y, Nakamura Y, Ohira M, *et al*. *PPP3CB* contributes to poor prognosis through activating nuclear factor of activated T-cells signaling in neuroblastoma. Molecular Carcinogenesis. 2019; 58: 426–435.

[14] Pfluger PT, Kabra DG, Aichler M, Schriever SC, Pfuhlmann K, García VC, *et al*. Calcineurin Links Mitochondrial Elongation with Energy Metabolism. Cell Metabolism. 2015; 22: 838–850.

[15] Chen L, He Q, Liu Y, Wu Y, Ni D, Liu J, *et al*. *PPP3CB* Inhibits Migration of G401 Cells via Regulating Epithelial-to-Mesenchymal Transition and Promotes G401 Cells Growth. International Journal of Molecular Sciences. 2019; 20: 275.

[16] Dotto GP. Calcineurin signaling as a negative determinant of keratinocyte cancer stem cell potential and carcinogenesis. Cancer Research. 2011; 71: 2029–2033.

[17] Golias T, Kery M, Radenkovic S, Papandreou I. Microenvironmental control of glucose metabolism in tumors by regulation of pyruvate dehydrogenase. International Journal of Cancer. 2019; 144: 674–686.

[18] Weisshaar N, Madi A, Cui G. Early TCR Signaling Sweetens Effector Function through PDHK1. Trends in Endocrinology and Metabolism: TEM. 2018; 29: 595–597.

[19] Chatterjee N, Pazarentzos E, Mayekar MK, Gui P, Allegakoen DV, Hrustanovic G, *et al*. Synthetic Essentiality of Metabolic Regulator PDHK1 in PTEN-Deficient Cells and Cancers. Cell Reports. 2019; 28: 2317–2330.e8.

[20] Peng F, Wang JH, Fan WJ, Meng YT, Li MM, Li TT, *et al*. Glycolysis gatekeeper PDK1 reprograms breast cancer stem cells under hypoxia. Oncogene. 2018; 37: 1062–1074.

[21] Kinnaird A, Dromparis P, Saleme B, Gurtu V, Watson K, Paulin R, *et al*. Metabolic Modulation of Clear-cell Renal Cell Carcinoma with Dichloroacetate, an Inhibitor of Pyruvate Dehydrogenase Kinase. European Urology. 2016; 69: 734–744.
[22] Golias T, Papandreou I, Sun R, Kumar B, Brown NV, Swanson BJ, *et al*. Hypoxic repression of pyruvate dehydrogenase activity is necessary for metabolic reprogramming and growth of model tumours. Scientific Reports. 2016; 6: 31146.
[23] Kim CJ, Tambe Y, Mukaisho KI, Sugihara H, Kageyama S, Kawauchi A, *et al*. Periostin suppresses *in vivo* invasiveness via PDK1/Akt/mTOR signaling pathway in a mouse orthotopic model of bladder cancer. Oncology Letters. 2017; 13: 4276–4284.
[24] Bersin RM, Stacpoole PW. Dichloroacetate as metabolic therapy for myocardial ischemia and failure. American Heart Journal. 1997; 134: 841–855.
[25] Hanahan D, Weinberg RA. Hallmarks of cancer: the next generation. Cell. 2011; 144: 646–674.
[26] Vander Heiden MG, Cantley LC, Thompson CB. Understanding the Warburg effect: the metabolic requirements of cell proliferation. Science (New York, N.Y.). 2009; 324: 1029–1033.
[27] Levine AJ, Puzio-Kuter AM. The control of the metabolic switch in cancers by oncogenes and tumor suppressor genes. Science (New York, N.Y.). 2010; 330: 1340–1344.
[28] Cao D, Qi Z, Pang Y, Li H, Xie H, Wu J, *et al*. Retinoic Acid-Related Orphan Receptor C Regulates Proliferation, Glycolysis, and Chemoresistance via the PD-L1/ITGB6/STAT3 Signaling Axis in Bladder Cancer. Cancer Research. 2019; 79: 2604–2618.
[29] Wang JZ, Zhu W, Han J, Yang X, Zhou R, Lu HC, *et al*. The role of the HIF-1α/ALYREF/PKM2 axis in glycolysis and tumorigenesis of bladder cancer. Cancer Communications (London, England). 2021; 41: 560–575.
[30] Nygren PJ, Scott JD. Regulation of the phosphatase PP2B by protein-protein interactions. Biochemical Society Transactions. 2016; 44: 1313–1319.
[31] Chen BK, Huang CC, Chang WC, Chen YJ, Kikkawa U, Nakahama KI, *et al*. PP2B-mediated dephosphorylation of c-Jun C terminus regulates phorbol ester-induced c-Jun/Sp1 interaction in A431 cells. Molecular Biology of the Cell. 2007; 18: 1118–1127.
[32] Luo L, Zhang Z, Qiu N, Ling L, Jia X, Song Y, *et al*. Disruption of FOXO3a-miRNA feedback inhibition of IGF2/IGF-1R/IRS1 signaling confers Herceptin resistance in HER2-positive breast cancer. Nature Communications. 2021; 12: 2699.
[33] Vasu S, McClenaghan NH, McCluskey JT, Flatt PR. Cellular responses of novel human pancreatic β-cell line, 1.1B4 to hyperglycemia. Islets. 2013; 5: 170–177.
[34] Wang JJ, Siu MK, Jiang YX, Leung TH, Chan DW, Cheng RR, *et al*. Aberrant upregulation of PDK1 in ovarian cancer cells impairs $CD8^+$ T cell function and survival through elevation of PD-L1. Oncoimmunology. 2019; 8: e1659092.
[35] Fujiwara S, Kawano Y, Yuki H, Okuno Y, Nosaka K, Mitsuya H, *et al*. PDK1 inhibition is a novel therapeutic target in multiple myeloma. British Journal of Cancer. 2013; 108: 170–178.
[36] Zhu J, Zheng G, Xu H, Jin X, Tang T, Wang X. Expression and prognostic significance of pyruvate dehydrogenase kinase 1 in bladder urothelial carcinoma. Virchows Archiv: an International Journal of Pathology. 2020; 477: 637–649.
[37] Korotchkina LG, Patel MS. Mutagenesis studies of the phosphorylation sites of recombinant human pyruvate dehydrogenase. Site-specific regulation. The Journal of Biological Chemistry. 1995; 270: 14297–14304.
[38] James MO, Jahn SC, Zhong G, Smeltz MG, Hu Z, Stacpoole PW. Therapeutic applications of dichloroacetate and the role of glutathione transferase zeta-1. Pharmacology & Therapeutics. 2017; 170: 166–180.
[39] Woolbright BL, Choudhary D, Mikhalyuk A, Trammel C, Shanmugam S, Abbott E, *et al*. The Role of Pyruvate Dehydrogenase Kinase-4 (PDK4) in Bladder Cancer and Chemoresistance. Molecular Cancer Therapeutics. 2018; 17: 2004–2012.